ISA Transactions ■ (■■■■) ■■■–■■■

Contents lists available at ScienceDirect

ISA Transactions

journal homepage: www.elsevier.com/locate/isatrans

Practice article

Improved fault ride through capability of DFIG based wind turbines using synchronous reference frame control based dynamic voltage restorer

A. Rini Ann Jerin *, Palanisamy Kaliannan, Umashankar Subramaniam

School of Electrical Engineering, VIT University, Vellore 632014, Tamil Nadu, India

ARTICLE INFO

Article history:
Received 3 November 2016
Received in revised form
18 May 2017
Accepted 29 June 2017

Keywords:
Doubly fed induction generator (DFIG)
Fault ride through (FRT)
Low voltage ride through (LVRT)
Dynamic voltage restorer (DVR)
Synchronous reference frame (SRF) control

ABSTRACT

Fault ride through (FRT) capability in wind turbines to maintain the grid stability during faults has become mandatory with the increasing grid penetration of wind energy. Doubly fed induction generator based wind turbine (DFIG-WT) is the most popularly utilized type of generator but highly susceptible to the voltage disturbances in grid. Dynamic voltage restorer (DVR) based external FRT capability improvement is considered. Since DVR is capable of providing fast voltage sag mitigation during faults and can maintain the nominal operating conditions for DFIG-WT. The effectiveness of the DVR using Synchronous reference frame (SRF) control is investigated for FRT capability in DFIG-WT during both balanced and unbalanced fault conditions. The operation of DVR is confirmed using time-domain simulation in MATLAB/Simulink using 1.5 MW DFIG-WT.

1. Introduction

The rise in level of wind penetration into the power grid is transforming the way the wind farms are operated. The large penetration of wind power has made it equivalent to conventional power plants and therefore expected to present enhanced immunity characteristic during grid voltage disturbances [1]. They are also expected to support the grid during system faults and recover soon in order to maintain the grid stability. Comparing to other requirements in wind power, Fault ride through (FRT) capability is the most demanding and is given major focus due to the rising grid penetration of wind energy and the recent advances in grid codes [2]. The wind farms connected to grid are mandatorily required to stay connected even during balanced or unbalanced voltage sags during system faults and support the grid through reactive power generation during fault period. Failing to support the grid or sudden disconnection of wind farms during faults may lead to severe consequences in grid and will exacerbate the problem [3]. Hence, ride through capability of wind turbines is being highlighted and the countries with largely growing wind energy capacity have started to mandate the FRT capability in wind farms which were installed without this FRT provision [4].

The FRT capability is imposed to maintain the wind turbine to remain stable and connected to the grid during grid side faults [5]. The FRT grid codes will differ in each country based on the Transmission system operator (TSO) requirements and therefore is country specific based on its grid behavior [6]. The FRT grid codes of some major countries are shown in Fig. 1. From this figure, it is clear that each country has different values of minimum voltage which is referred as the V_{fault} and the time up to which this voltage should be sustained is denoted by T_{fault} and the voltage up to which it has to be recovered is the $V_{recovery}$ within a time of $T_{recovery}$. For example in Germany, according to E.ON grid codes the V_{fault} is up to 0 pu for a T_{fault} of 150 ms and has to reach $V_{recovery}$ of 0.9 pu within a $T_{recovery}$ of 1500 ms. Therefore, one control cannot be applicable to all countries and for all types of wind generators. In a country like India, where grid is generally weak, it will require more reactive power support during grid faults with the increasing wind energy penetration [7]. The country has made the amendment for mandatory changes in the recent times and therefore a wind turbine type specific study becomes very essential for the current scenario [8].

Among the wind generators, Doubly fed induction generator (DFIG) is popular for its partially rated converters which have the ability to operate with decoupled active and reactive power control, it's reduced cost, weight, size and losses compared to full power converter based system [9]. But DFIG-WTs are very sensitive to disturbances in grid voltages especially voltage sags [10]. Abrupt voltage

Abbreviations: DFIG-WT, Doubly fed induction generator based wind turbine; DVR, Dynamic voltage restorer; FCL, . Fault current limiter; FRT., Fault ride through; GSC, .Grid side converter; IDVR, Interline dynamic Voltage Restorer; LVRT, Low voltage ride through; PCC, Point of common coupling; PLL, Phase locked loop; PWM, Pulse width modulation; RSC, Rotor side converter; SDR, Series dynamic resistor; SGSC, Series grid side converter; SFCL, Superconducting fault current limiter; SRF, Synchronous reference frame; STATCOM, Static synchronous compensator; TSO, Transmission system operator; VSC, Voltage source converter

* Corresponding author.
E-mail addresses: riniannjerin@gmail.com (A. Rini Ann Jerin), kpalanisamy@vit.ac.in (P. Kaliannan), umashankar.s@vit.ac.in (U. Subramaniam).

http://dx.doi.org/10.1016/j.isatra.2017.06.029
0019-0578/

Nomenclature

V_{fault}	Fault voltage
$V_{recovery}$	Recovery voltage
T_{fault}	Fault time
$T_{recovery}$	Recovery time
v_{ds}, v_{qs}	Stator dq voltages
v_{dr}, v_{qr}	Rotor dq voltages
i_{ds}, i_{qs}	Stator dq currents
i_{dr}, i_{qr}	Rotor dq currents
I_s	Stator current
I_r	Rotor current
ω_e	Supply angular frequency
ω_r	Rotor angular frequency
λ_{ds}, λ_{qs}	dq stator flux linkages
λ_{dr}, λ_{qr}	dq rotor flux linkages
R_s, R_r	Stator and rotor resistance
L_s, L_r	Stator and rotor inductance
L_{ls}, L_{lr}	Stator and rotor leakage inductance
L_m	Magnetizing inductance
P_s	Stator active power
Q_s	Stator reactive power
V_1, V_2	Nominal and fault line voltage values
V_N	Nominal grid voltage
ε	Sag depth
V_{DVR}	DVR voltage rating
P_{DVR}	DVR power rating
I_{load}, I'_{load}	Load current before sag and after sag
V_{grid} , V'_{grid}	Grid voltage before sag and after sag
V_{load}, V'_{load}	Load voltage before sag and after sag
ψ	Phase angle difference between load current and grid voltage
δ	Phase jump
v_L^*	Reference load voltage
v_{La}, v_{Lb}, v_{Lc}	Load abc voltages
v_{La}^*, v_{Lb}^*, v_{Lc}^*	Reference abc load voltages
v_{Ld}, v_{Lq}, v_{L0}	Load dq voltages
v_{Ld}^*, v_{Lq}^*	Reference dq load voltages
v_{sd}, v_{sq}	Supply voltages at PCC
v_{sd}^*, v_{sq}^*	Reference supply voltages
v_{L0}	Zero sequence component of load voltage
v_{Dd}, v_{Dq}	DVR voltages
v_{Dd}^*, v_{Dq}^*, v_{D0}^*	DVR reference voltages
v_{dvra}, v_{dvrb}, v_{dvrc}	DVR abc voltages
v_{dvra}^*, v_{dvrb}^*, v_{dvrc}^*	Reference DVR abc voltages

sags can cause over-voltage and over-currents in the rotor windings which is capable of destroying the rotor windings, if not provided with proper protection devices. Conventionally crowbars were installed for the protection of rotor windings to disconnect the rotor converters and absorb the over-currents. But installation of crowbar leads to absorption of reactive power and also stalls the generation of active power [11]. This further contributes to the grid collapse during voltage sag conditions. The over-current in the rotor during voltage sag increases the voltage in DC bus, oscillations in the stator and rotor currents, also disturbances in active and reactive power of DFIG-WT. Also in any active control based crowbar with DFIG-WT, the Grid side converter (GSC) can be set to control the reactive power and voltage at Point of common coupling (PCC) [12]. But the smaller rating of GSC, is not sufficient to provide reactive power support for grid fault in case of a weak grid. This can cause voltage instability in the grid. Therefore, Static synchronous compensator (STATCOM) for FRT was proposed to generate reactive power and to support DFIG-WT [13]. But STATCOM cannot protect the Rotor side converter (RSC) and therefore it has to be operated along with the crowbar to protect RSC from rotor over-currents during grid fault. Other solutions proposed include the Series dynamic resistance (SDR) in the stator or rotor side or using Series grid side converter (SGSC) topology [14].

Other methods include Fault current limiter (FCL) based FRT in DFIG-WT have fast quenching time but have the disadvantage of high construction cost [15]. Superconducting fault current limiter (SFCL) is also receiving more attention for providing FRT capability in DFIG-WTs as discussed in [16–18]. Advancements in DVR are widely discussed as follows like the transformer less DVR by incorporating multilevel cascaded H-bridge inverter is discussed in [19]. The quality of the compensation voltage of a DVR improved by multilevel inverter concept is discussed in [20], by providing wide correction range using bidirectional energy control. Several DVR connected in series with a common DC-link called as Interline dynamic voltage restorer (IDVR) is discussed in [21]. The reactive power injection capability of DVR considering the load voltage constraints is discussed in [22]. Recently, these advancements in DVR are getting incorporated for improving the FRT capability in DFIG-WT.

It is suggested that use of external power electronic device to compensate the faulty grid voltage will eliminate the need for any additional protection device for DFIG-WT. Dynamic Voltage restorer (DVR) is a series compensation device which injects the appropriate compensating voltage to correct the faulty grid voltage [23]. The Voltage source converter (VSC) plays a major role in the operation of DVR is investigated using various control schemes to verify the efficiency of the voltage restoration [24]. The magnitude and phase angle of the injected voltage varies depending on the sag parameters. The performance of the DVR can be improved based on the control and compensation technique utilized. The operation of DVR for FRT capability is normally tested for the voltage sag and swell compensation of the wind turbine in distribution systems. But DVR is capable of sag, swell and harmonic compensation and can be represented as a "multifunctional DVR" [25,26]. It is found that the compensation of unbalanced voltage sags using DVR is effective, only when the controller is able to compensate the negative sequence component of the grid voltage. Different DVR control strategies have been developed for improving the operation and performance of the voltage compensation [27]. DVR based FRT augmentation has been applied for Squirrel cage induction generators [28]. The improvement in FRT capability performance of DFIG-WTs with DVR requires further investigation with change in DVR control adoption [29]. Effective operation in mitigating sag, swell and harmonics using reduced rating of DVR with Synchronous reference frame (SRF) control is discussed only for non-linear load in [30]. The operation of DVR using SRF control for improving the FRT capability in DFIG-WT has not been discussed so far.

In this paper, improved FRT Capability of DFIG-WTs using SRF control based DVR is presented. Generally, harmonic compensation capability of DVR is not focused based on SRF control operation during FRT capability improvement. The FRT capability of a 1.5 MW DFIG-WT using 1.5 MVA DVR is simulated and the results are carried out for balanced and unbalanced voltage sag conditions. Also, the harmonic compensation is also tested and the % THD values using SRF and conventional Feed-forward control is compared. The improvement in stator voltage, stator current, rotor current and DC-link voltage using SRF control is discussed. The contribution in active and reactive power support provided by DFIG-WT and DVR during FRT is also focused.

Please cite this article as: Rini Ann Jerin A, et al. Improved fault ride through capability of DFIG based wind turbines using synchronous reference frame control based dynamic voltage restorer. ISA Transactions (2017), http://dx.doi.org/10.1016/j.isatra.2017.06.029

The remaining section of this article is as follows: Section 2 deals with the modeling of DFIG-WT and DVR. The operation of the two control techniques and its comparison is given in Section 3. The control is simulated and tested for balanced and unbalanced sags and also for harmonic mitigation using MATLAB/Simulink and is discussed in Section 4 and the Section 5 ends with conclusion.

2. Operation of DVR with DFIG-WT

DVR is a series interface scheme connected to the DFIG-WT to address the voltage sag issue and to comply with the FRT capability of wind turbines. DVR is capable of voltage sag, swell and harmonic compensation but very much concentrated for the voltage sag compensation capability while installing for the ride through capability of wind turbines. DFIG-WT is especially sensitive to grid disturbances and hence FRT capability is essential to allow it to operate without tripping and comply with grid codes. DFIG-WT with series compensation of DVR to support the ride through capability and improve the transient stability operation is shown in Fig. 2. The DVR is installed at the PCC to inject voltage in series to continue the operation of DFIG-WT through active power and reactive power support to the grid for recovering from the fault. The improvement in the performance of DVR while operating with conventional Feed-forward and SRF based control is compared and also analyzed for harmonic compensation. This will help to ensure the FRT capability and also to improve the power quality of the grid operating with integrated wind generators.

2.1. Modeling of DFIG based wind turbine system

Understanding the transient changes in DFIG-WT operation during grid faults is necessary in order to carry out further studies on how to overcome the voltage sag during fault [31]. The stator of DFIG-WT is connected directly to the grid and rotor is connected to the grid via slip rings through the RSC and GSC. The converter connected to the rotor side is the RSC and connected to the grid side is the GSC which together constitutes only up to 30–35% of the total capacity of the machine. Therefore, popularly known as partially rated converters and are responsible for the four quadrant operation of the converter's Pulse width modulation (PWM) which attributes to the controllable voltage and frequency. The controllable voltage and frequency provides the variable speed operation of the generator, thereby proving constant output from the generator during fluctuating wind speeds. Whereas the stator remains constant at fundamental frequency, even when the generator operates at different speeds. The advantage of harnessing more power by employing the variable speed operation of DFIG-WT is the reason for the popularity of this generator type. It can extend the slip up to ± 0.3 pu and therefore can still generate power without falling in the nonlinear part of its characteristic curve [32]. Fig. 3 shows 'T-form' equivalent circuit of the DFIG-WT. The DFIG-WT operates in the popular stator-flux-oriented-vector control which is structured in a double-closed-loop strategy. The outer power control can do the decoupled independent active and reactive power control and the inner power control with feed-forward decoupling parts can control the rotor current. The d-axis of the synchronous frame is aligned with the stator-flux space vector in the field oriented control which rotates at the speed of ω_s in anti-clockwise direction [33]. Since the stator- flux oriented vector control is applied, the RSC controls the active and reactive power of the DFIG-WT and the GSC maintains the DC-link voltage as constant.

The most indispensable parameters for consideration during sag condition in DFIG-WT are the stator voltage, rotor current and the DC-link voltage [34]. During balanced fault, it causes a large transient over-current regardless of the recovery type. This transient overshoot is due to the natural response of the stator flux and decays within 0.1 s. The RSC regains control and regulates back to pre-fault value. Whereas unbalanced fault causes steady-state ripple during fault due to the negative sequence component. Large over-currents will cause sudden increase of active power from RSC which cannot be transferred by the GSC due to its partial rating, therefore causes a rise in DC-link voltage up to 1.2 pu. Further, the power transfer capacity through GSC reduces due to the low voltage during fault. The over-currents in the rotor and the sudden rise in DC-link voltage will be cleared after fault and this clearance varies with respect to the recovery type. Transients that occur during fault clearing instant are lesser than the fault occurring instant due to the better capability of GSC with the availability of nominal voltage. These transients during fault clearance can be controlled by taking the circuit breaker parameter constraints into account. Also, full voltage recovery in one step using a

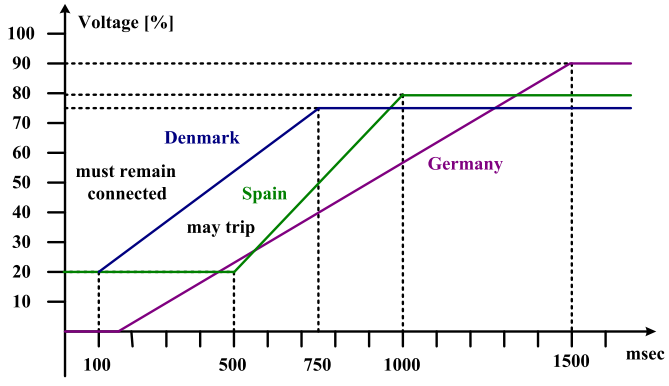

Fig. 1. Fault ride through grid codes of various countries.

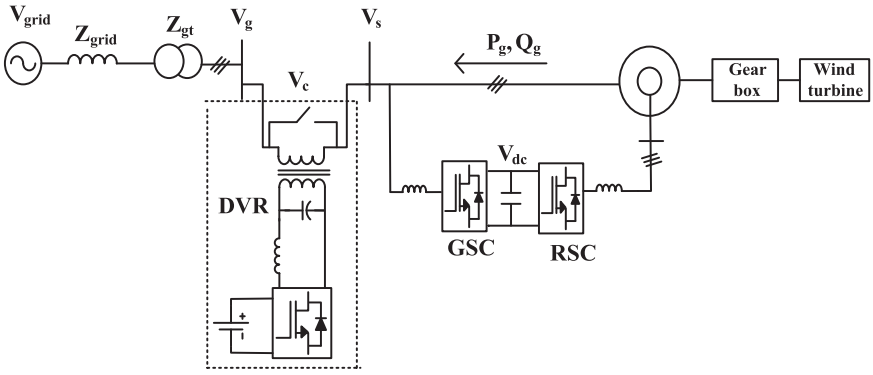

Fig. 2. Schematic diagram of FRT capability in DFIG with DVR.

Please cite this article as: Rini Ann Jerin A, et al. Improved fault ride through capability of DFIG based wind turbines using synchronous reference frame control based dynamic voltage restorer. ISA Transactions (2017), http://dx.doi.org/10.1016/j.isatra.2017.06.029

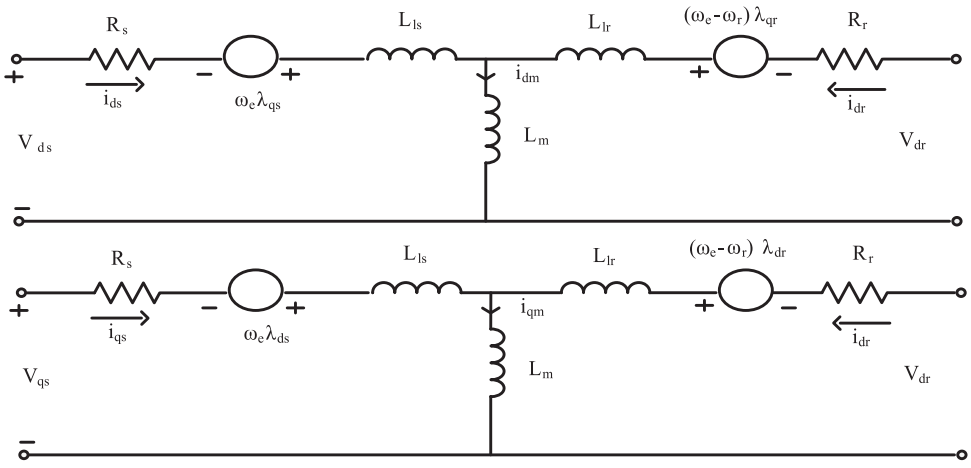

Fig. 3. 'T-form' equivalent circuit of DFIG.

circuit breaker causes large change in stator-forced flux and which will require a large natural flux component.

However, the response is different for unbalanced fault condition due to the negative sequence component. There is no transient overshoot during fault occurring instant but there is a large current ripple in the rotor winding, double-frequency oscillations in the DC-link voltage and negative sequence oscillations remain unsuppressed during fault. Any phase jump in the supply voltage during unbalanced voltage sag due to fault will cause excessive transients due to the negative sequence components. Large phase angle jumps can cause severe detrimental effects on the transient response of DFIG-WT. Therefore, the modeling of DFIG-WT behavior during grid faults is done using the 'T-form' equivalent circuit of DFIG-WT as shown in Fig. 3.

The stator and the rotor voltage in the synchronous dq reference frame are as given below. The expressions of flux, voltages and currents are as in [15].

$$v_{ds} = R_s i_{ds} + \frac{d\lambda_{ds}}{dt} - \omega_e \lambda_{qs} \tag{1}$$

$$v_{qs} = R_s i_{qs} + \frac{d\lambda_{qs}}{dt} + \omega_e \lambda_{ds} \tag{2}$$

$$v_{dr} = R_r i_{dr} + \frac{d\lambda_{dr}}{dt} - (\omega_e - \omega_r)\lambda_{qr} \tag{3}$$

$$v_{qr} = R_r i_{qr} + \frac{d\lambda_{qr}}{dt} + (\omega_e - \omega_r)\lambda_{dr} \tag{4}$$

Here, v_{ds}, v_{qs} are dq stator voltages and v_{dr}, v_{qr} are dq rotor voltages. i_{ds}, i_{qs} are dq stator currents and i_{dr}, i_{qr} are dq rotor currents. ω_e is the supply angular frequency and ω_r is the rotor angular frequency. λ_{ds}, λ_{qs} are the dq stator flux linkages and λ_{dr}, λ_{qr} is the dq rotor flux linkages. R_s and R_r are the stator and rotor resistance respectively.

$$L_s = L_{ls} + L_m \tag{5}$$

$$L_r = L_{lr} + L_m \tag{6}$$

Here, L_s and L_r are the stator and rotor inductance respectively. L_{ls} and L_{lr} are the stator and rotor leakage inductance respectively and L_m is the magnetizing inductance.

$$\lambda_{ds} = L_s i_{ds} + L_m i_{dr} \tag{7}$$

$$\lambda_{qs} = L_s i_{qs} + L_m i_{qr} \tag{8}$$

$$\lambda_{dr} = L_m i_{ds} + L_r i_{dr} \tag{9}$$

$$\lambda_{qr} = L_m i_{qs} + L_r i_{qr} \tag{10}$$

In stator flux-oriented control, q-axis rotor current component controls the stator active power (P_s) and rotor d-axis current component controls the stator reactive power (Q_s) respectively.

$$P_s = \frac{3}{2}(v_{qs} i_{qs} + v_{ds} i_{ds}) \tag{11}$$

$$Q_s = \frac{3}{2}(v_{qs} i_{ds} - v_{ds} i_{qs}) \tag{12}$$

The threshold values of rotor current and DC-link voltage are essential to ensure efficient FRT capability. The threshold value of the rotor current during fault is 1.5 pu to 2 pu values. Also, the DC-link voltage rating is 1150 V and its threshold value is 1.35 pu [35]. The DVR operation should maintain the values of rotor current and DC-link voltage within these safety limits.

2.2. Modeling of dynamic voltage restorer (DVR)

The DVR is a VSC connected in series to the grid and DFIG-WT at PCC to inject the appropriate compensating voltage to correct the voltage sag, swell or harmonics and obtain the nominal stator voltage. The switching signals to the VSC are given by the PWM technique with the appropriate controller. The DVR compensates the faulty line voltage to allow the DFIG-WT to continue its nominal operation as demanded by the grid codes. Conventional Phase locked loop (PLL) which is also in the synchronous dq reference frame detects the grid phase angle and utilized for synchronization. In-phase compensation method is utilized for both Feed-forward and SRF control of DVR. Since, the grid codes demand compensation of full voltage sag during fault conditions, DVR is rated for the power of the wind turbine [23]. For voltage sags with zero-phase angle jump, the active power requirement of DVR is given by

$$P_{DVR} = \left(\frac{V_1 - V_2}{V_1}\right) P_{load} \tag{13}$$

V_1 is the nominal line voltage and V_2 is the fault line voltage values.

Also, the DVR voltage rating (V_{DVR}) depends mainly on the voltage sag depth which requires compensation. The required

Please cite this article as: Rini Ann Jerin A, et al. Improved fault ride through capability of DFIG based wind turbines using synchronous reference frame control based dynamic voltage restorer. ISA Transactions (2017), http://dx.doi.org/10.1016/j.isatra.2017.06.029

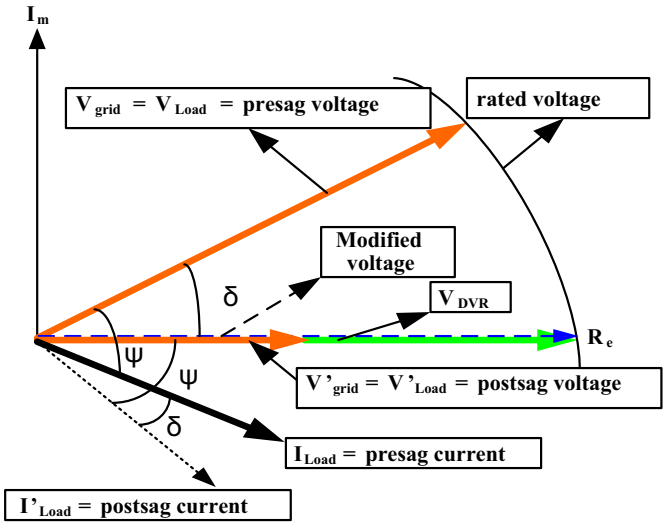

Fig. 4. Phasor diagram for in-phase compensation of voltage using DVR.

voltage amplitude with in-phase compensation is given by

$$V_{DVR} = V_1 \varepsilon \tag{14}$$

Here, V_1 is the nominal line voltage, I_1 is the nominal line current and ε is the sag depth. The value of active power calculated based on the vector diagram in Fig. 4. is given below.

$$P_{DVR} = \sqrt{3} V_{DVR} I_1 * \varepsilon * \cos\psi \tag{15}$$

Here, ψ is the phase angle difference between load current (I_{load}) and grid voltage (V_{grid}) both before sag and difference between (I'_{load}) and (V'_{grid}) after sag. δ is the phase jump between load voltage before sag and after sag (between V_{load}, V'_{load}) and phase jump of the load current before sag and after sag (between I_{load}, I'_{load}) as in Fig. 4.

The injection transformer must be adequately designed and an appropriate transformer ratio has to be chosen. Higher rating of the transformer is essential to avoid the risk of high inrush currents and saturation which is discussed in [36,37].

3. Control techniques of DVR

3.1. Feed-forward control strategy

Generally, DVR can be controlled by either open-loop control [24] or closed loop control. The operation of a conventional open-loop controller of DVR in synchronous reference frame, which is also called as a Feed-forward control is shown in Fig. 5. The $V_{dref} = V_0$ is the reference controlled by the required magnitude of the load bus voltage respectively. The primary control structure depends on the supply voltage and its phase angle to calculate the required modulation depth of the voltage to be injected. But this control does not include the feedback which will take into account the voltage drop across the filter inductor and transformer. The operation of the control in the synchronous dq-reference frame allows simpler clamping of the injection voltage. Therefore, enables DVR to partially compensate deep voltage sags and to maintain the sinusoidal injection voltage profile. The operation of control is synchronized to the supply voltage through PLL which is essential to maintain smooth output voltage even during phase jump. The control generates the dq reference which is transformed to three phase stationary frame value in order to generate the PWM modulation signals [38,39].

3.2. Synchronous reference frame (SRF) control

The Synchronous reference frame (SRF) control used for detecting the sag and generating the appropriate reference for triggering the IGBT is discussed in [30]. This control includes the feedback control of the reference load voltage v_L^* which is derived and converted to rotating reference frame using abc-dq0 by Park's transformation using the sinθ, cosθ unit vectors from PLL. When the rotating frame is aligned 90 degrees behind "a" axis, the following relations are as follows.

$$\begin{bmatrix} v_{Lq} \\ v_{Ld} \\ v_{L0} \end{bmatrix} = \frac{2}{3} \begin{bmatrix} \cos\theta & \cos\left(\theta - \frac{2\pi}{3}\right) & \cos\left(\theta + \frac{2\pi}{3}\right) \\ \sin\theta & \sin\left(\theta - \frac{2\pi}{3}\right) & \sin\left(\theta + \frac{2\pi}{3}\right) \\ \frac{1}{2} & \frac{1}{2} & \frac{1}{2} \end{bmatrix} \begin{bmatrix} v_{La}^* \\ v_{Lb}^* \\ v_{Lc}^* \end{bmatrix} \tag{16}$$

$$v_{Dd} = v_{Sd} - v_{Ld} \tag{17}$$

$$v_{Dq} = v_{Sq} - v_{Lq} \tag{18}$$

$$v_{Dd}^* = v_{Sd}^* - v_{Ld} \tag{19}$$

$$v_{Dq}^* = v_{Sq}^* - v_{Lq} \tag{20}$$

The reference calculated by subtracting the load voltage from supply voltage is used to regulate by using two PI controllers. The load voltage in abc frame are (v_{La}, v_{Lb}, v_{Lc}) and reference load voltage in abc frame are (v_{La}^*, v_{Lb}^*, v_{Lc}^*). The load voltages in dq frame are load voltages (v_{Ld}, v_{Lq}, v_{L0}) and the reference load voltage in dq frame is (v_{Ld}^*, v_{Lq}^*). The supply voltage at PCC in rotating dq frame is (v_{sd}, v_{sq}) and the reference supply voltage is (v_{sd}^*, v_{sq}^*). The parameter with subscript zero denotes the zero sequence components.

$$\begin{bmatrix} v_{dvra}^* \\ v_{dvrb}^* \\ v_{dvrc}^* \end{bmatrix} = \frac{2}{3} \begin{bmatrix} \cos(\theta) & \sin(\theta) & \\ \cos\left(\theta - \frac{2\pi}{3}\right) & \sin\left(\theta - \frac{2\pi}{3}\right) & 1 \\ \cos\left(\theta + \frac{2\pi}{3}\right) & \sin\left(\theta + \frac{2\pi}{3}\right) & 1 \end{bmatrix} \begin{bmatrix} v_{Dq}^* \\ v_{Dd}^* \\ v_{D0}^* \end{bmatrix} \tag{21}$$

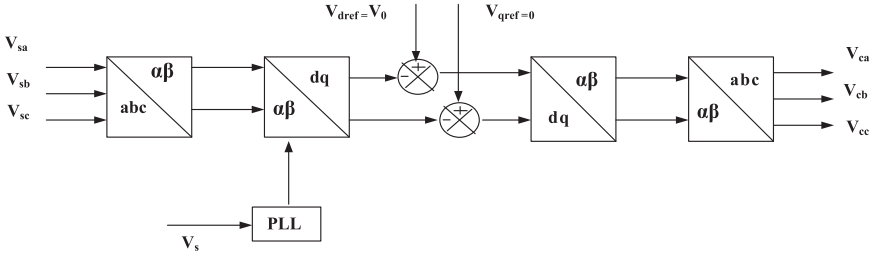

Fig. 5. Block diagram of Feed-forward control.

Please cite this article as: Rini Ann Jerin A, et al. Improved fault ride through capability of DFIG based wind turbines using synchronous reference frame control based dynamic voltage restorer. ISA Transactions (2017), http://dx.doi.org/10.1016/j.isatra.2017.06.029

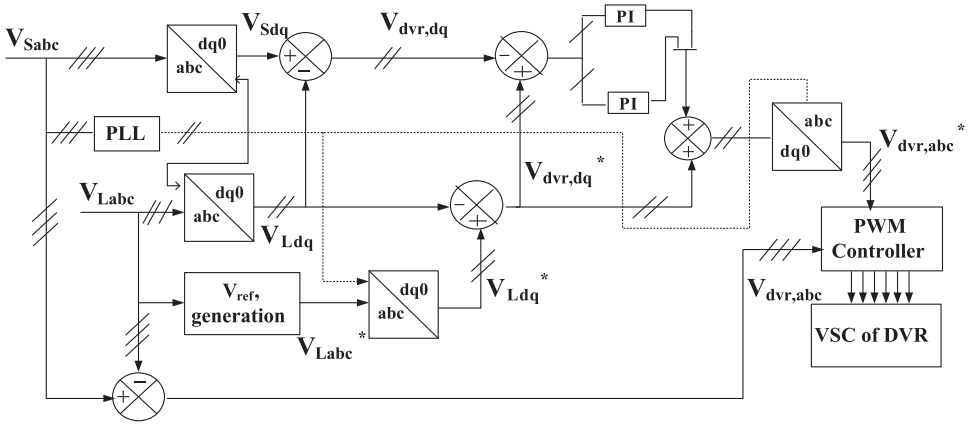

Fig. 6. Block diagram of SRF control.

Table 1
Comparison of DVR controller parameter and performance features.

	Feed-forward control	SRF control
Operating frame	Synchronous frame (dq)	Synchronous frame (dq)
Digital operation	2 dq operations	4 dq operations
Tuning	–	K_p, K_i
Stability	Unstable for negative sequence components	Stable
Robustness	Does not allow dynamics	Robust to dynamic changes
Number of controllers	–	2 PI control
Control complexity	Simple	Relatively complex (require PI gain values)

DVR voltages in rotating dq frame are: DVR voltage (v_{Dd}, v_{Dq}), DVR reference voltage $(v^*_{Dd}, v^*_{Dq}, v^*_{D0})$. DVR voltage in abc frame are actual DVR voltage $(v_{dvra}, v_{dvrb}, v_{dvrc})$, reference DVR voltage $(v^*_{dvra}, v^*_{dvrb}, v^*_{dvrc})$. These are used to generate the PWM pulses to the VSC which is operated at 10 kHz. The SRF control is as shown in Fig. 6 and the error between the DVR reference and actual voltage is minimized by two PI controls. Since this control adopts a voltage feedback by including the load voltage value, it minimizes the steady-state error in the fundamental component. The resonances are damped by adding the LC filter components [7].

The general parameters of the Feed-forward and SRF control are compared in Table 1.

4. Simulation Results with performance comparison and discussion

The FRT capability is tested using simulation for a 1.5 MW wind turbine with DFIG-WT which is connected to an infinite bus with a DVR connected at PCC through circuit breaker in MATLAB/Simulink environment. For full compensation of full voltage sag, DVR

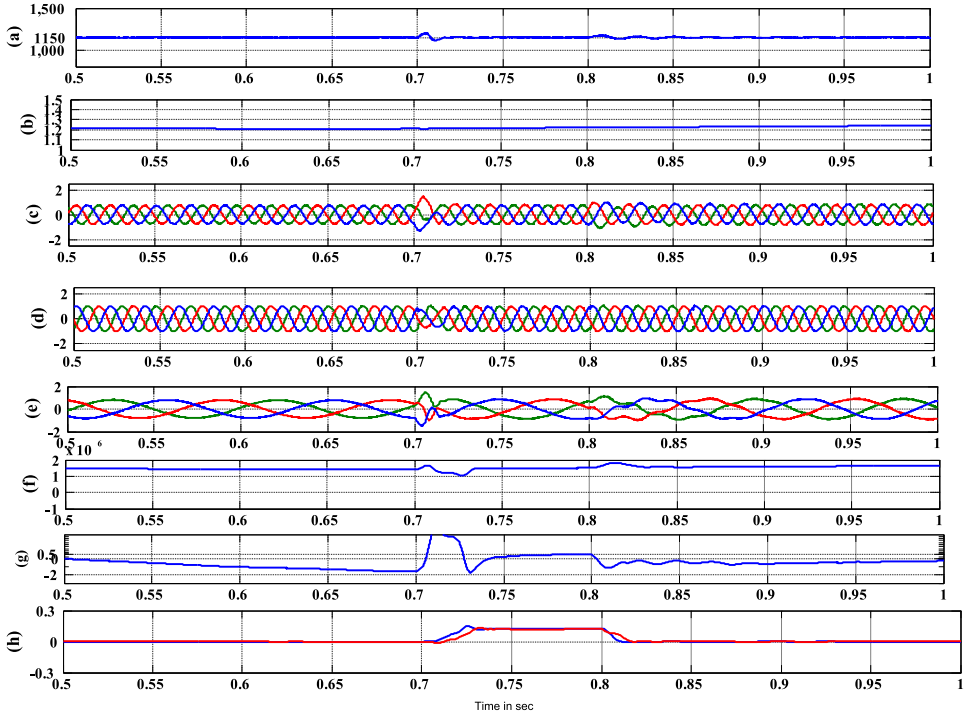

Fig. 7. Results for balanced sag between 0.7 and 0.8 s using SRF control (from top to bottom) (a). Dc link voltage in Volts, (b). Rotor speed in pu, (c). Stator current in pu, (d). Stator voltage in pu, (e). Rotor current in pu, (f). Active power of DFIG in MW, (g) reactive power of DFIG in MVAR, (h) active and reactive power of DVR in blue and red respectively in pu.

Please cite this article as: Rini Ann Jerin A, et al. Improved fault ride through capability of DFIG based wind turbines using synchronous reference frame control based dynamic voltage restorer. ISA Transactions (2017), http://dx.doi.org/10.1016/j.isatra.2017.06.029

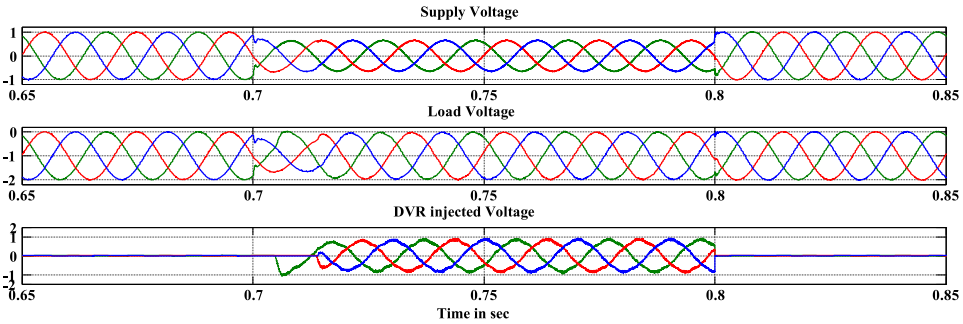

Fig. 8. Results for voltage sag mitigation using DVR with SRF control for balanced sag between 0.7 and 0.8 s for 0.35 pu sag.

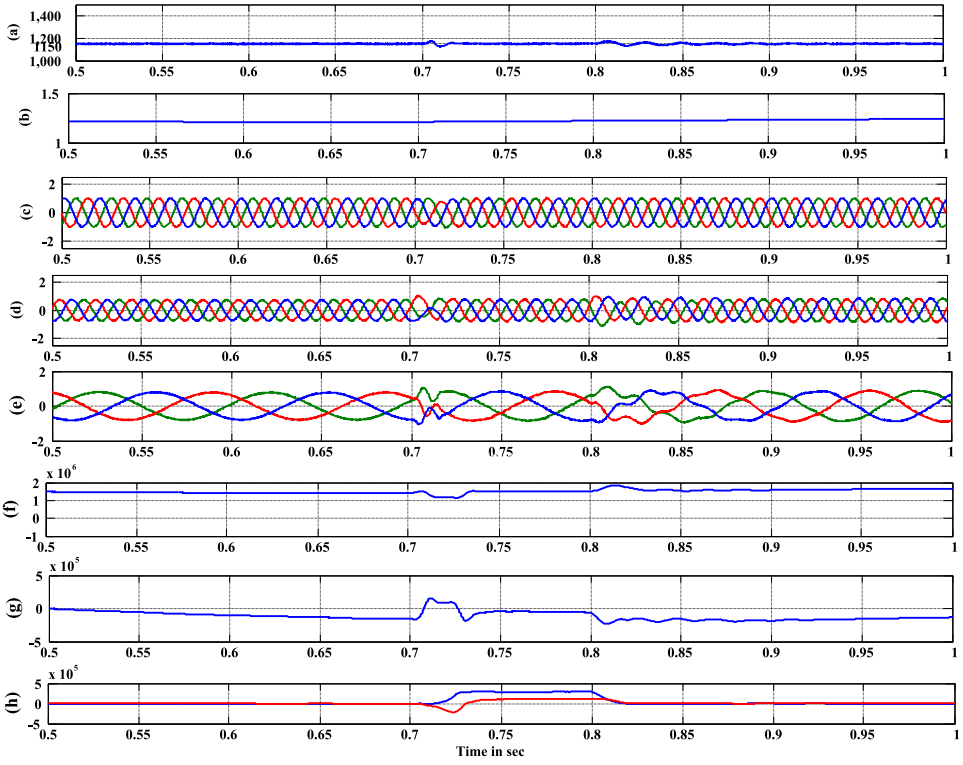

Fig. 9. Results for unbalanced sag using SRF control between 0.7 and 0.8 s (from top to bottom) (a). Dc link voltage in Volts, (b). Rotor speed in pu, (c). Stator current in pu, (d). Stator voltage in pu, (e). Rotor current in pu, (f). Active power of DFIG in MW, (g) reactive power of DFIG in MVAR, (h) active and reactive power of DVR in blue and red respectively in pu.

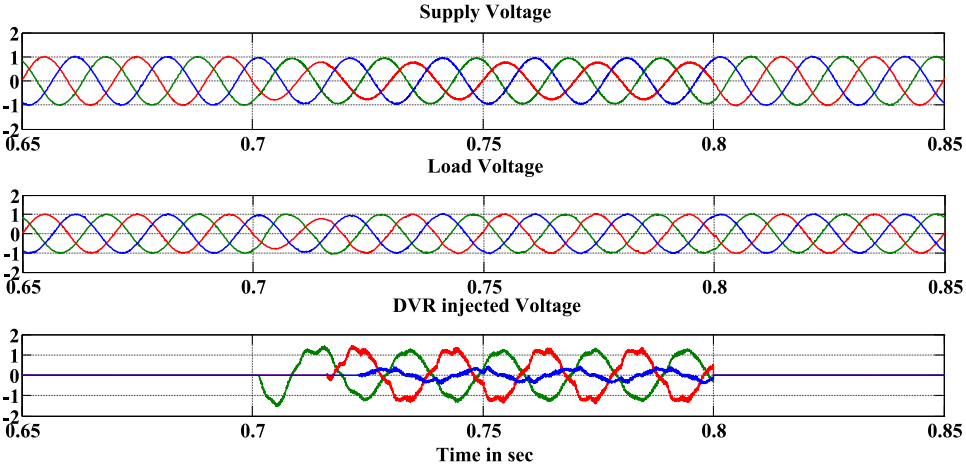

Fig. 10. Results for voltage sag mitigation using DVR with SRF control for unbalanced sag between 0.7 and 0.8 s for 0.35 pu sag.

Please cite this article as: Rini Ann Jerin A, et al. Improved fault ride through capability of DFIG based wind turbines using synchronous reference frame control based dynamic voltage restorer. ISA Transactions (2017), http://dx.doi.org/10.1016/j.isatra.2017.06.029

Table 2
Simulation parameters of DFIG.

Rated power of DFIG	1.5 MW
Cut-in speed, cut-out speed	6 m/s, 30 m/s
Rated wind speed	11 m/s
Stator voltage/frequency	575 V/ 50 Hz
Stator resistance	0.023 pu
Rotor resistance	0.016 pu
Stator leakage inductance	0.18 pu
Rotor leakage inductance	0.16 pu
Generator inertia constant	0.685
Nominal DC bus voltage	1150 V
Gains of *d-axis* PI controller(K_p, K_i)	$K_{p1} = 0.5$, $K_{i1} = 0.35$
Gains of *q-axis* PI controller(K_p, K_i)	$K_{p2} = 0.5$, $K_{i2} = 0.35$

Table 3
Simulation parameters of DVR.

Capacity	1.5 MVA
Filter inductance	0.1 mH
Filter capacitance	1 μF
Switching frequency	10 kHz
Series transformer	1.5 MVA, 230/340 V

Table 4
Comparison of THD values for the Feed-forward and SRF control.

%THD values	DVR with Feed-Forward control	DVR with SRF control
Supply voltage	30%	30%
Supply current	5.18%	1.34%
Load voltage	5.24%	1.35%
Load current	5.18%	1.34%

has to be rated for the power of the wind turbine, therefore 1.5 MVA power rating DVR is chosen. The DVR is connected through a 1.5 MVA series transformer with 230/340 V rating windings. The simulation is tested for a short-duration balanced three-phase-to-ground fault and unbalanced single-phase-to ground fault. The SRF control of DVR is used primarily to compensate the voltage sags to augment the FRT capability of DFIG-WT as per grid codes. The operation of DVR control is also verified for harmonic compensation and to evaluate the efficiency based on the harmonic order of the voltage. The system response for balanced and unbalanced three phase voltage sag is tested for 100 ms between 0.7 s and 0.8 s. The voltage sag is a reduction of 35% from the nominal value of voltage. The grid frequency is 50 Hz and voltage is 120 kV which is connected through transformers and has 575 V at PCC where DVR and DFIG-WT are connected. The converter switching frequency is 10 kHz.

The performance of the DVR is investigated for SRF control in order to achieve proper FRT operation. The SRF control utilizes PI controllers with PLL for synchronization; therefore it has fast transient response compared to the conventional Feed-forward control under balanced and distorted conditions. The response of control for constant wind speed at 11 m/s is maintained since the effect of fault is for very short duration of 100 ms, which does not allow noticeable speed variations. Fig. 7 clearly shows the performance of DFIG-WT during balanced sag for 0.35 pu for 5 cycles during 0.7 s to 0.8 s. The measured signal in Fig. 7(a) and (b) show that the DC-link voltage does not exceed the threshold value and is maintained constant at 1150 V and the rotor speed is maintained constant at 1.2 pu respectively. Fig. 7(c), (d) and (e) show that the stator current, stator voltage and rotor current are effectively mitigated with very minimum disturbance respectively. Fig. 7 (f) shows that the nominal operation of DFIG-WT is maintained by continuing the active power generation of DFIG-WT at 1.5 MW. Fig. 7(g) shows that DVR provides the reactive power support to DFIG-WT during fault condition and Fig. 7(h) shows both active and reactive power of DVR. Fig. 8 shows the DVR operation during the same balanced fault condition and the sub-figures shows the mitigation capability of DVR. Fig. 9 clearly shows the performance of DFIG-WT during unbalanced sag for 0.35 pu for 5 cycles during 0.7 s to 0.8 s. The FRT operation during unbalanced condition shows similar performance improvement for all parameters as explained briefly in Fig. 7. Single-phase unbalance in phase A is shown in Fig. 10 during the fault condition. The operation of DVR mitigation during the unbalanced fault condition is clearly shown.

The Table 2 gives the parameters of DFIG-WT and Table 3 gives the parameters of DVR used in the simulation. Increased transient response of FRT capability is necessary to comply with the grid codes. The increased transient stability is important for the operation of DFIG-WT during these sudden disturbances. The sudden disturbance causes high stator currents I_s and rotor currents I_r. Using DVR the stator currents and rotor currents are maintained with distortions, but still the RSC is kept in operation. Therefore, the RSC is able to control the active and reactive power independently. Therefore, the speed is kept constant and reactive power is generated as per grid codes using DVR. Thus, the unacceptable high rotor currents during fault are mitigated to avoid any damage to rotor and to continue its operation. The other important measurements of the active power, reactive power, DC-link voltage, rotor speed, stator voltage, stator current and rotor current are shown in Fig. 7 and Fig. 9 for balanced and unbalanced faults respectively. The fault mitigation and harmonic mitigation shows the effective operation of DFIG-WT using DVR with SRF control. The SRF control reduces the %THD from 5.18% of Feed-forward control to 1.34% which proves the enhanced performance of the control in abiding with harmonic standards and maintains grid codes.

The comparison of the performance of the controllers in improving the DVR operation is very essential. This will in turn help in understanding the actual operation and stability improvement in DFIG-WT during FRT operation using DVR. The harmonic

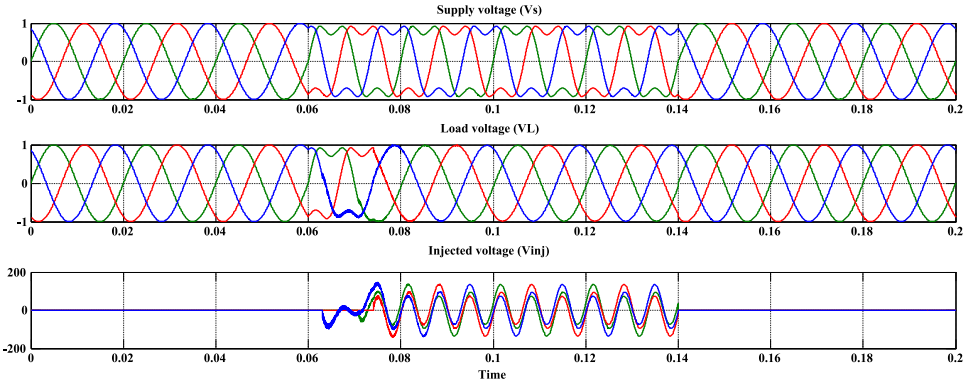

Fig. 11. Harmonic mitigation of DVR with Feed-forward control for harmonics in the supply voltage sag between 0.06 s and 0.14 s.

Please cite this article as: Rini Ann Jerin A, et al. Improved fault ride through capability of DFIG based wind turbines using synchronous reference frame control based dynamic voltage restorer. ISA Transactions (2017), http://dx.doi.org/10.1016/j.isatra.2017.06.029

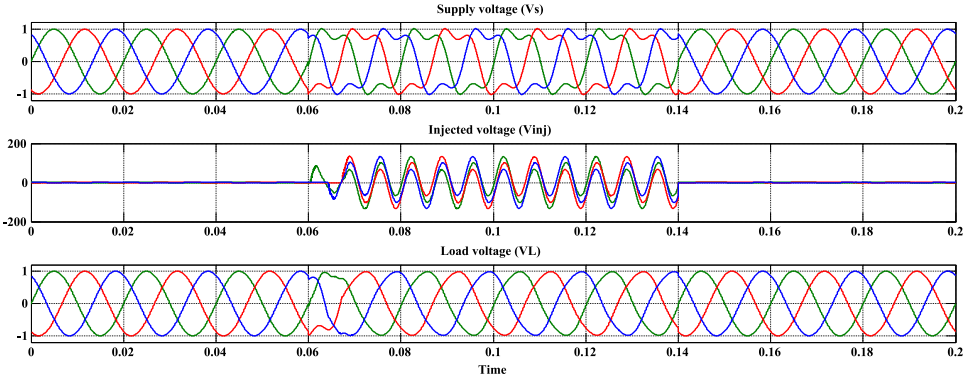

Fig. 12. Harmonic mitigation of DVR with SRF control for harmonics in the supply voltage sag between 0.06 s and 0.14 s.

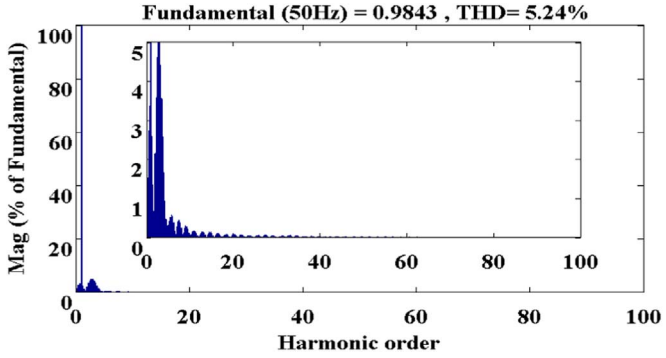

Fig. 13. Harmonic spectrum of DVR Load voltage with Feed forward control.

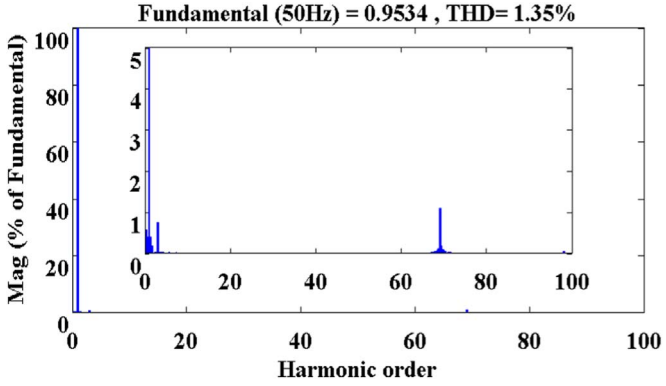

Fig. 14. Harmonic spectrum of DVR Load voltage with SRF control within IEEE 519 standard.

compensation ability of both controllers in terms of % THD value is discussed as shown in Table 4. The harmonics are injected along the source side in the simulation for the understanding of the DVR controller ability in mitigating the lower order harmonics. The Fig. 11 and Fig. 12 show the harmonic mitigation of DVR using Feed-forward control and SRF control respectively for 30% of third order harmonics in supply voltage between 0.06 s and 0.14 s. The harmonic order comparison as per Fig. 13 and Fig. 14 shows that SRF control of DVR is capable of mitigating harmonics and maintains the %THD within the IEEE 519 standard. From the results and discussion, the following points are concluded.

1) The improvement in stator voltage, stator current, rotor current and DC-link voltage of DFIG-WT during fault conditions can be easily observed from the results. (Fig. 7, Fig. 9)
2) In the case of active power, effective active power evacuation of 1.5 MW generated by DFIG-WT during the fault conditions is carried out with lesser oscillation.
3) Reactive power support is a challenging grid code requirement for FRT during voltage recovery. Using SRF controlled DVR provides better reactive power injection.
4) SRF control has shown performance improvement in the case excellent reactive power compensation, load balancing and good harmonic mitigation.
5) The %THD values using SRF and conventional Feed-forward control is compared and found to have better harmonic compensation ability.

5. Conclusion

The FRT capability of wind turbines are essential with the growing integration of wind power in the grid and contribute to the reliable grid integration. There are several countries which have recently imposed the mandatory guidelines for FRT capability implementation in already installed and operating grid connected wind turbines. Therefore this paper investigates the performance of DVR with SRF control for the FRT capability of DFIG-WTs. The control performance is compared with Feed-forward control which is operated with the same synchronous reference frame. The performance of the controllers is compared for the voltage sag mitigation during balanced and unbalanced grid faults. The harmonic mitigation capability of DVR is also discussed. The comparison of harmonic compensation of both controllers in terms of % THD shows that SRF control provides better performance. The performance comparison suggests that the operation of DVR is suitable for FRT capability as per grid code standards imposed globally. Simulation results show better performance of DVR with SRF control for improving the FRT capability of DFIG-WT.

Acknowledgement

The authors would like to thank the management of VIT University for the support in carrying out this research work. This research did not receive any specific grant from funding agencies in the public, commercial, or not-for-profit sectors.

References

[1] Li YW, Blaabjerg F, Vilathgamuwa DM, Loh PC. Design and comparison of high performance stationary-frame controllers for DVR implementation. IEEE Trans Power Electron 2007;22:602–12. http://dx.doi.org/10.1109/TPEL.2006.890002.
[2] Jadhav HT, Roy R. A comprehensive review on the grid integration of doubly fed induction generator. Int J Electr Power Energy Syst 2013;49:8–18. http://dx.doi.org/10.1016/j.ijepes.2012.11.020.
[3] Sorensen P, Unnikrishnan AK, Mathew SA. Wind farms connected to weak grids in India. Wind Energy 2001;4:137–49. http://dx.doi.org/10.1002/we.52.

Please cite this article as: Rini Ann Jerin A, et al. Improved fault ride through capability of DFIG based wind turbines using synchronous reference frame control based dynamic voltage restorer. ISA Transactions (2017), http://dx.doi.org/10.1016/j.isatra.2017.06.029

[4] Xu L, Wang Y. Dynamic modeling and control of DFIG-based wind turbines under unbalanced network conditions. IEEE Trans Power Syst 2007;22:314–23. http://dx.doi.org/10.1109/TPWRS.2006.889113.

[5] Singh B, Singh SN. Development of grid connection requirements for wind power generators in India. Renew Sustain Energy Rev 2011;15:1669–74. http://dx.doi.org/10.1016/j.rser.2010.11.026.

[6] Ibrahim A, Nguyen T, Lee D, Kim S. A fault ride-through technique of DFIG wind turbine systems using dynamic voltage restorers. Energy Convers IEEE Trans 2011;26:871–82. http://dx.doi.org/10.1109/TEC.2011.2158102.

[7] Rini Ann Jerin A, Palanisamy K, Umashankar S, Thirumoorthy AD. Power quality improvement of grid connected wind farms through voltage restoration using dynamic voltage restorer. Int J Renew Energy Res 2016;6:53–60. http://dx.doi.org/10.1234/ijrer.v6i1.3070.

[8] Suppioni VP, Grilo AP, Teixeira JC. Control methodology for compensation of grid voltage unbalance using a series-converter scheme for the DFIG. Electr Power Syst Res 2016;133:198–208. http://dx.doi.org/10.1016/j.epsr.2015.12.034.

[9] Justo JJ, Mwasilu F, Jung J-W. Enhanced crowbarless FRT strategy for DFIG based wind turbines under three-phase voltage dip. Electr Power Syst Res 2017;142:215–26. http://dx.doi.org/10.1016/j.epsr.2016.09.029.

[10] Rolán A, Pedra J, Córcoles F. Detailed study of DFIG-based wind turbines to overcome the most severe grid faults. Int J Electr Power Energy Syst 2014;62:868–78. http://dx.doi.org/10.1016/j.ijepes.2014.05.031.

[11] Pannell G, Atkinson DJ, Zahawi B. Minimum-threshold crowbar for a fault-ride-through grid-code-compliant DFIG wind turbine. IEEE Trans Energy Convers 2010;25:750–9. http://dx.doi.org/10.1109/TEC.2010.2046492.

[12] Hossain MK, Ali MH. Transient stability augmentation of PV/DFIG/SG-based hybrid power system by parallel-resonance bridge fault current limiter. Electr Power Syst Res 2016;130:89–102. http://dx.doi.org/10.1016/j.epsr.2015.08.016.

[13] Ananth DVN, Nagesh Kumar GV. Fault ride-through enhancement using an enhanced field oriented control technique for converters of grid connected DFIG and STATCOM for different types of faults. ISA Trans 2016;62:2–18. http://dx.doi.org/10.1016/j.isatra.2015.02.014.

[14] Castilla M, miret j, Camacho A, Matas J, Garcia de Vicuna L. Voltage Support control strategies for static synchronous compensators under unbalanced voltage sags. Ind Electron IEEE Trans 2014;61:808–20. http://dx.doi.org/10.1109/TIE.2013.2257141.

[15] Alaraifi S, Moawwad A, El Moursi MS, Khadkikar V. Voltage booster schemes for fault ride-through enhancement of variable speed wind turbines. IEEE Trans Sustain Energy 2013;4:1071–81. http://dx.doi.org/10.1109/TSTE.2013.2267017.

[16] Chen L, Chen H, Yang J, Zhu L, Tang Y, Koh LH, et al. Comparison of superconducting fault current limiter and dynamic voltage restorer for LVRT improvement of high penetration microgrid. IEEE Trans Appl Supercond 2017;27:1–7. http://dx.doi.org/10.1109/TASC.2017.2656624.

[17] Guo W, Xiao L, Dai S. Fault current limiter-battery energy storage system for the doubly-fed induction generator : analysis and experimental verification; 2016, 10. p. 653–660. doi:10.1049/iet-gtd.2014.1158.

[18] Rashid G, Member S, Ali MH, Member S. Nonlinear control-based modified BFCL for LVRT capacity enhancement of DFIG based wind farm; 2016, 8969. p. 1–12. doi:10.1109/TEC.2016.2603967.

[19] Prabaharan N, Palanisamy K. A comprehensive review on reduced switch multilevel inverter topologies, modulation techniques and applications. Renew Sustain Energy Rev 2017;76:1248–82. http://dx.doi.org/10.1016/j.rser.2017.03.121.

[20] Cao J, Liu H, Ding P, Yang B, Xie S. Wide correction range three-level dynamic voltage corrector. IEEE Trans Power Electron 2016;31:6217–25. http://dx.doi.org/10.1109/TPEL.2015.2501827.

[21] Shahabadini M, Hossein Iman-Eini. Improving the performance of a cascaded H-bridge-based interline dynamic voltage restorer. IEEE Trans Power Deliv 2016;31:1160–7. http://dx.doi.org/10.1109/TPWRD.2015.2480967.

[22] Rold J, Member S, Ochoa-gim M, Zamora-macho JL. On the power-flow limits and control in series-connected custom power devices. IEEE Trans Power Electron 2016;31:7328–38. http://dx.doi.org/10.1109/TPEL.2015.2509003.

[23] Wessels C, Gebhardt F, Fuchs FW. Fault ride-through of a DFIG wind turbine using a dynamic voltage restorer during symmetrical and asymmetrical grid faults. IEEE Trans Power Electron 2011;26:807–15. http://dx.doi.org/10.1109/TPEL.2010.2099133.

[24] Padiyar KR. FACTS controllers in power transmission and distribution. New Age International; 2007.

[25] İnci M, Bayındır KÇ, Tümay M. Improved Synchronous Reference Frame based controller method for multifunctional compensation. Electr Power Syst Res 2016;141:500–9. http://dx.doi.org/10.1016/j.epsr.2016.08.033.

[26] Khodabakhshian A, Mahdianpoor M, Hooshmand R. Robust control design for multi-functional DVR implementation in distribution systems using quantitative feedback theory. Electr Power Syst Res 2013;97:116–25. http://dx.doi.org/10.1016/j.epsr.2012.12.015.

[27] Mohanty A, Viswavandya M, Ray PK, Patra S. Stability analysis and reactive power compensation issue in a microgrid with a DFIG based WECS. Int J Electr Power Energy Syst 2014;62:753–62. http://dx.doi.org/10.1016/j.ijepes.2014.05.033.

[28] Jiang F, Tu C, Shuai Z, Xiao F, Lan Z. Combinational voltage booster technique for fault ride-through capability enhancement of squirrel-cage induction generator. Electr Power Syst Res 2016;136:163–72. http://dx.doi.org/10.1016/j.epsr.2016.02.010.

[29] Senthil Kumar N, Gokulakrishnan J. Impact of FACTS controllers on the stability of power systems connected with doubly fed induction generators. Int J Electr Power Energy Syst 2011;33:1172–84. http://dx.doi.org/10.1016/j.ijepes.2011.01.031.

[30] Jayaprakash P, Singh B, Kothari DP, Chandra A, Al-Haddad K. Control of reduced-rating dynamic voltage restorer with a battery energy storage system. IEEE Trans Ind Appl 2014;50:1295–303. http://dx.doi.org/10.1109/TIA.2013.2272669.

[31] Mohseni M, Islam SM, Masoum MAS. Impacts of symmetrical and asymmetrical voltage sags on DFIG-Based wind turbines considering phase-angle jump, voltage recovery, and sag parameters. IEEE Trans Power Electron 2011;26:1587–98. http://dx.doi.org/10.1109/TPEL.2010.2087771.

[32] Hemami A. Wind turbine technology. Cengage Learning; 2012 24.

[33] Pena R, Clare JC, Asher GM. Doubly fed induction generator using back-to-back PWM converters and its application to variable-speed wind-energy generation. IEE Proc - Electr Power Appl 1996;143:231. http://dx.doi.org/10.1049/ip-epa:19960288.

[34] Seman S, Niiranen J, Kanerva S, Arkkio A, Saitz J. Performance study of a doubly fed wind-power induction generator under network disturbances. IEEE Trans Energy Convers 2006;21:883–90. http://dx.doi.org/10.1109/TEC.2005.853741.

[35] Justo JJ, Mwasilu F, Jung J-W. Doubly-fed induction generator based wind turbines: a comprehensive review of fault ride-through strategies. Renew Sustain Energy Rev 2015;45:447–67. http://dx.doi.org/10.1016/j.rser.2015.01.064.

[36] Huang PH, El Moursi MS, Xiao W, Kirtley JL. Novel fault ride-through configuration and transient management scheme for doubly fed induction generator. IEEE Trans Energy Convers 2013;28:86–94. http://dx.doi.org/10.1109/TEC.2012.2222886.

[37] Sasitharan S, Mishra MK, Kumar BK, Jayashankar V. Rating and design issues of DVR injection transformer. Conf Proc - IEEE Appl Power Electron Conf Expo - APEC 2008:449–55. http://dx.doi.org/10.1109/APEC.2008.4522760.

[38] Rahimi M, Parniani M. Dynamic behavior analysis of doubly-fed induction generator wind turbines – The influence of rotor and speed controller parameters. Int J Electr Power Energy Syst 2010;32:464–77. http://dx.doi.org/10.1016/j.ijepes.2009.09.017.

[39] Rahimi M, Parniani M. Low voltage ride-through capability improvement of DFIG-based wind turbines under unbalanced voltage dips. Int J Electr Power Energy Syst 2014;60:82–95. http://dx.doi.org/10.1016/j.ijepes.2014.02.035.

Please cite this article as: Rini Ann Jerin A, et al. Improved fault ride through capability of DFIG based wind turbines using synchronous reference frame control based dynamic voltage restorer. ISA Transactions (2017), http://dx.doi.org/10.1016/j.isatra.2017.06.029